DESIGN AND DEVELOPMENT OF THREE-DEGREES-OF-FREEDOM ROBOTIC ARM FOR ELECTRIC VEHICLE CHARGING STATION

Article history
Received
4th November 2024
Received in revised form
5th December 2024
Accepted
5th December 2024
Published
26th December 2024

*Corresponding author
nursafwati@utm.my

Muhammad Nor Syamsulyusri Ruslan[a], Hendri Maja Saputra[b] , Nur Safwati Mohd Nor[a*]

[a] Faculty of Mechanical Engineering, Universiti Teknologi Malaysia 81310 Johor Bahru, Johor, Malaysia
[b] Research Center for Smart Mechatronics, National Research and Innovation Agency, Jl.Cisitu, No.21/154D, Bandung 40135, Indonesia

ABSTRACT

The exponential growth of the electric vehicle (EV) industry requires the development of more efficient and easily accessible charging infrastructures. The existing manual charging procedures provide significant difficulties, especially for those with impairments. The objective of this project was to overcome these difficulties by designing and developing a robotic arm that is particularly designed for automating the process of charging electric vehicles. The project aimed to improve operational efficiency and user accessibility by designing a three-degrees-of-freedom robotic arm using CAD software, SOLIDWORKS, and prototyping it using 3D printing technology. The main approaches employed were thorough Finite Element Analysis (FEA) to guarantee the structural integrity to confirm the operational dependability. The primary results indicate that the robotic arm design successfully automates the charging process, resulting in a substantial reduction in the human labor needed from users and an improvement in the accuracy of the charging connection. These results not only showcase the arm's capacity to completely transform EV charging methods but also emphasize its flexibility in different vehicle settings, indicating a wide range of possible uses in automated systems in the future.

KEYWORDS

Robotic Arm, EV charging, FEA, 3-DOF

INTRODUCTION

The exponential rise of the electric vehicle (EV) industry requires the creation of more efficient and easily accessible charging infrastructures to accommodate this increase. The existing manual charge procedures provide substantial difficulties, especially for those with impairments. The objective of this research is to overcome these difficulties by creating a robotic arm with three degrees of freedom that is particularly designed for automating the process of charging electric vehicles. This will improve the efficiency of operations and make it easier for users to access the charging process [1].

Although robotic arms have found success in areas including manufacturing, healthcare, and services, their potential for automating the EV charging process has not been thoroughly investigated. The absence of study in this area emphasizes a noteworthy potential to utilize robotic technology to tackle the difficulties linked to conventional EV charging techniques. The current manual charging techniques are frequently burdensome and require physical effort, discouraging user engagement and presenting specific difficulties for individuals with impairments [2].

This project aims to create, build, and verify a robotic arm that can automate the process of connecting and disconnecting at electric vehicle charging stations. This study entails a meticulous design procedure employing sophisticated computer-aided design (CAD) tools and creating prototypes using 3D printing. The assessment of the prototypes is conducted through simulation to ensure their durability and effectiveness. The technique is intended to validate the feasibility of the robotic arm in real-life situations, therefore facilitating future technical progress in electric vehicle infrastructure.

METHODOLOGY

Design Generation

The objective of this project is to design a 3 DOF robotic arm to automate the charging process of electric vehicles. The robotic arm can reach a maximum distance of 758mm and can hold weight up to 0.1kg. The design of the proposed robot arm is shown in Figure 1.

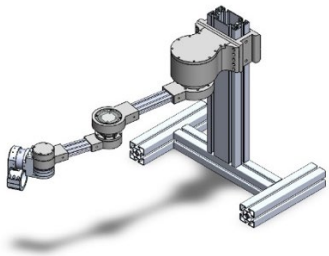

Figure 1: 3 DOF robotic arm design

Motor Selection

The motor selection considered not only the operational torque requirements but also potential transient and dynamic torque demands arising from specific motion profiles. Torque margins were evaluated to ensure that peak demands during high-acceleration phases could be handled by the selected motor. The formula used to calculate the torque is:

$$Torque, T = Moment\ of\ inertia, I \times angular\ acceleration\ , \alpha \quad (1)$$

Where moment of inertia,

$$I = mass\ (m)\ \times\ distance\ (r) \times\ distance\ (r) \quad (2)$$

Distance, r = distance between rotational axis to the centre of mass of arm.

For this calculation, the robot arm was set to rotate from rest at 0° to 90° to reach the target and each arm will complete rotation in 2 seconds. The FBD of the robot arm is shown in Figure 2. Therefore, to find the angular acceleration for the robot arm, kinematics motion was applied as below:

$$\theta_f - \theta_i = \omega_0 t\ \times \frac{1}{2}\alpha t^2 \quad (3)$$

Where θ_i=0 and ω_0=0.

$$90^\circ = \frac{\pi}{2} rad \text{ and } 0^\circ = 0\ rad \quad (4)$$

$$\frac{\pi}{2} - 0 = (0)(2) \times \frac{1}{2}\alpha 2^2 \quad (5)$$

$$\alpha = \frac{\pi}{4} rads^{-1} \quad (6)$$

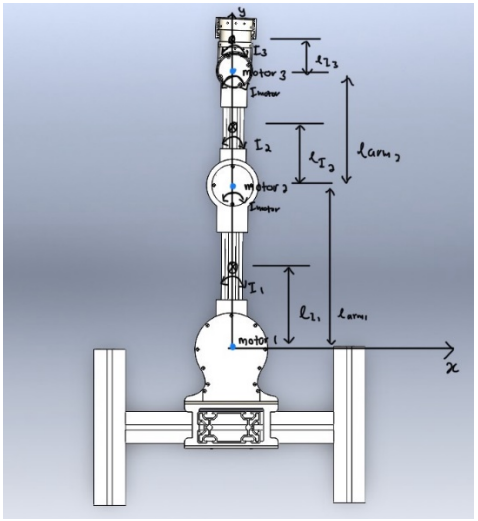

Figure 2: FBD of the robotic arm

For joint 1, the calculation will consider both arm 1 and arm 2, the motor at each joint with weight assumed at 500g, end effector, and the maximum payload weight of 250g considering the sagging of the robot arm. The calculation is shown below:

Arm 1:

$mass\ arm1 = 973.15\ g$
$distance = 161.88\ mm$
$motor = 500\ g$
$distance = 318.95\ mm$

$$I = \left[(0.97315 \times 0.16188^2) \times \frac{\pi}{4}\right] + \left[(0.5 \times 0.31895^2) \times \frac{\pi}{4}\right] = 0.060Nm$$

Arm 2:

$mass\ arm2 = 427.03\ g$
$distance = 453.19mm$
$motor = 500g$
$distance = 542.93mm$

$$I = \left[(0.42703 \times 0.45319^2) \times \frac{\pi}{4}\right] + \left[(0.5 \times 0.54293^2) \times \frac{\pi}{4}\right] = 0.185Nm$$

End-effector:

$mass\ end-effector = 526.60\ g$
$distance = 606.68mm$

$$I = (0.52660 \times 0.60668^2) \times \frac{\pi}{4} = 0.152Nm$$

Payload:

$payload = 250\ g$
$distance = 646.81mm$

$$I = (0.25 \times 0.64681^2) \times \frac{\pi}{4} = 0.082Nm$$

$$Total\ torque, T_T = T_{arm1} + T_{arm2} + T_{end-effector} + T_{payload} = 0.060 + 0.185 + 0.152 + 0.082 = 0.479Nm$$

The total torque for the joint 1 is 0.479Nm. However, a safety margin of 1.5 should account for any uncertainties in the calculation. Therefore, the final torque for joint 1 is:

$$T_{final} = T_T \times safety\ margin = 0.479Nm \times 1.5 = 0.7185Nm$$

For joint 2, the calculation is the same as joint 1 where arm2, end-effector, weight of motor assumed at 500g, and payload of 250g will be considered in the calculation. The calculation is shown below:

Arm 2:

$mass\ arm2 = 427.03\ g$
$distance = 134.24mm$
$motor = 500g$
$distance = 223.98mm$

$$I = \left[(0.42703 \times 0.13424^2) \times \frac{\pi}{4}\right] + \left[(0.5 \times 0.22398^2) \times \frac{\pi}{4}\right] = 0.026Nm$$

End-effector:

$end-effector = 526.60\ g$
$distance = 287.73mm$

$$I = (0.52660 \times 0.28773^2) \times \frac{\pi}{4} = 0.034Nm$$

Payload:

$payload = 250\ g$
$distance = 327.3mm$

$$I = (0.25 \times 0.3273^2) \times \frac{\pi}{4} = 0.021Nm$$

$$Total\ torque, T_T = T_{arm2} + T_{end-effector} + T_{payload} = 0.026 + 0.034 + 0.021 = 0.081Nm$$

Considering a safety margin of 1.5;

$$T_{final} = T_T \times safety\ margin = 0.081Nm \times 1.5 = 0.1215Nm$$

Based on this calculation, the torque required by arm 1 is 0.7185 Nm and arm 2 is 0.1215 Nm. As all the joints will be using the same motor to reduce design complexity, by considering the minimum torque required for the motor to rotate the arm is 0.7185 Nm the motor selected should have the holding torque larger than this value. Table 1 shows the comparison table of motors that are available in the market.

Table 1: Comparison of motor specification

Criteria	Nema 17 (40mm) Planetary Gear Ratio=1:5.18 Stepper Motor	NEMA 17HS4401 Bipolar Stepper Motor	Planetary DC Geared Servo Motor
Holding torque (Nm)	2.3	0.4	1.77
Max torque (Nm)	11.914	0.4	9.11

Motor Selection

With the selection of 3D printing as the method used in this project, two common materials are considered which are PLA and ABS. Table 2 shows the comparison of this material based on a few criteria. Based on this table, PLA is the best material to use in the fabrication process. Both PLA and ABS have good strength however, PLA is more rigid as compared to ABS which is crucial in this project to avoid deflection on the robotic arm. Furthermore, PLA also has a higher yield strength compared to ABS. Higher yield strength will impact a higher amount of stress the material can handle

before fracture which is very crucial in the robotic arm.

Table 2: Comparison of material between PLA and ABS

Property	PLA	ABS
Origin	Biodegradable and derived from renewable resources (like corn starch or sugarcane).	Petroleum-based plastic.
Strength	Good strength, but less than ABS.	Higher strength and toughness than PLA.
Flexibility	More rigid, and less flexible than ABS	More flexible and durable than PLA.
Print temperature	Lower printing temperature	Higher printing temperature
Tensile strength	Approx. 37-55 MPa	Approx. 27-52 MPa
Yield strength	Approx. 50-60MPa	Approx. 40-50 MPa
Cost	RM 0.20/gram	RM 0.50/gram

RESULTS AND DISCUSSIONS

Design Reflection and Modifications

Based on the initial concept of the robotic arm proposed, some modifications are required on the design to ensure a working robotic arm. The initial design was proposed to use the same motor for all the joints. However, the selected motor will have a significant impact on the stability of the robotic arm due to the weight of the motor itself. This results in a large deflection and failure on the robotic arm as shown in Figure 3.

Figure 3: Failure on the initial design

This failure is most likely due to the motor weight at the end-effector. Reselecting the motor will be the next step in ensuring this failure does not occur again. By using the formula in Equation (1), the new torque required to rotate the end-effector can be calculated. The weight of the printed parts will be scaled to ensure accurate weight since a lighter motor results in lower holding torque. The calculated torque to rotate the end-effector is 0.0665 Nm. Therefore, a motor that holds torque higher than this and has a low weight will be considered. Stepper motor 17HS4023 was chosen due to its holding torque of 0.13Nm and weight of 130g.

Design Analysis – Stress Analysis

Finite Element Analysis is a fundamental tool in engineering that allows design engineers to visually assess possible stress and strain, anticipate failures, and validate theoretical predictions. Integrating the FEA in this analysis not only validates the design but also enhances the reliability and safety of the structure. The use of the Von Mises stress criteria in this context is crucial for assessing whether the material will undergo plastic deformation under the specified loading circumstances.

Based on Figures 4 and 5, the color gradient of the contour plot ranges from blue which represents the lowest level of stress to red which represents the highest level of stress. This gradient allows for the quantification of stress intensity throughout the arm. The highest stress which is illustrated in red as shown in Figure 6 highlights the most critical areas in which the possible point of failure to happen. This area of high stress which is located at the middle joint of the arm is the most critical area that stress optimization might be necessary. The stress distribution is high intensity around the joint area which might be due to the significant mechanical load that is potentially due to the weight of the motor

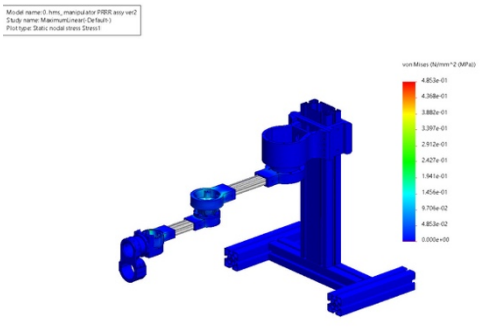

Figure 4: Von misses the contour plot

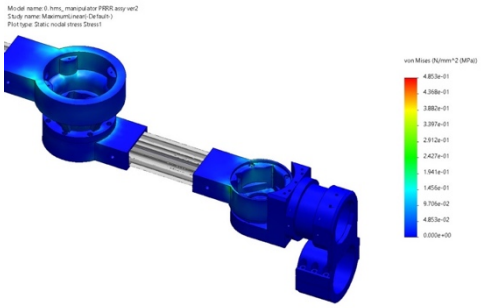

Figure 5: Critical area of stress distribution

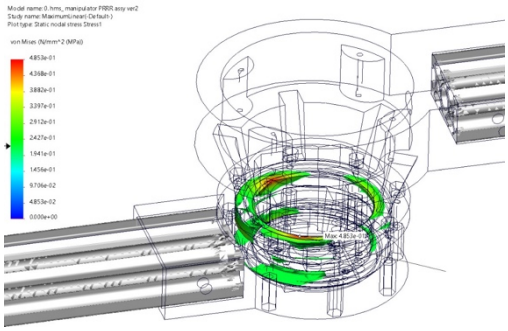

Figure 6: Highest von misses stress area

Based on the analysis, the areas with the highest levels of stress are primarily located at the joints. This is to be expected since the joints experience significant mechanical loads and moments. It is necessary to compare the highest recorded stress values with the yield strength of the materials employed in the design of the arm. From the analysis, the highest stress recorded was 0.4853 MPa and the material's yield strength is 49MPa. Since the highest stress does not exceed the yield strength of the material, the design can be considered as safe. However, these regions experiencing significant stress may still require evaluation for material optimization or geometric modification to improve the durability and operational lifespan of the robotic arm.

Design Analysis – Displacement Analysis

Figure 7 and Figure 8 show the displacement analysis of the robotic arm when applying the load. Conducting this analysis is vital for assessing the deformation of various components of the robotic arm when subjected to operational load. This is a critical aspect in guaranteeing the durability and functioning of the arm in real-world scenarios.
Both of these figures illustrate the displacement of particular parts of the robotic arm focusing more on its joints and the gripper mechanism. The displacements are highlighted using colors varying from blue to red which shows how much the robotic arm moves under applied forces. It is worth noting that, the red signalizes the highest point whereas the lowest would be signaled by blue color. For instance, in this case, the maximum displacement at the gripper end is approximately 14.19 mm, as shown by the red color. This analysis proposes that components highlighted in yellow and orange, which represent moderate displacement, have the potential to experience stress or strain at a level that can lead to fatigue during their regular usage. Therefore, it is crucial to accurately identify these displacement values to gain an understanding of the potential actions that would be done during actual operation, as well as to enable any necessary reinforcement or redesign of the robotic arm.

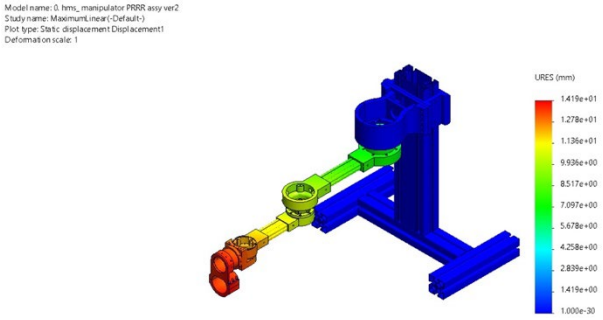

Figure 7: Displacement contour plot

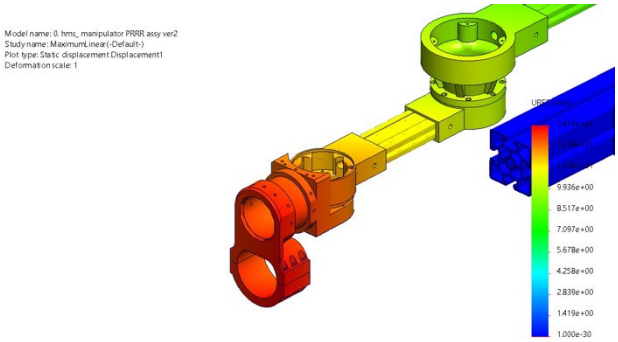

Figure 8: Highest displacement area

Design Analysis – Strain Analysis

In addition to stress, strain is another criterion for design analysis that should be evaluated. Strain refers to the deformation that takes place in a substance when it is exposed to external forces or stress. Strain is typically measured by dividing the amount of deformation by the initial length. Strain plays a critical role in finite element analysis since it allows for the evaluation of how materials will deform, either by stretching or compressing, under

certain operational circumstances. Figure 9 illustrates the strain distribution throughout the length of the robotic arm assembly as a whole. The visualization shows that certain sections show more strain than others, especially those near joints and connecting parts. These sections are vital to the arm's operational integrity since they take the greatest amount of mechanical motions. Figure 10 emphasizes crucial elements, such as joints, which experience the highest levels of strain, as illustrated by the red and orange areas. Elevated strain in these regions may suggest possible locations of structural failure or places prone to material fatigue over a period of time. The color gradient ranging from blue to green, yellow, and red indicates a shift from areas of lower strain to higher strain, illustrating the distribution and absorption of load inside the component. The highest strain recorded is 6.656E-5 which is located at the motor housing of arm 2.

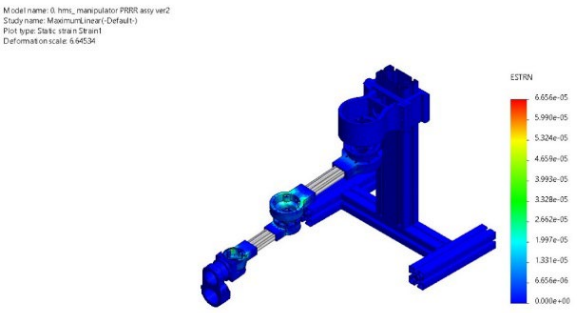

Figure 9: Strain contour plot

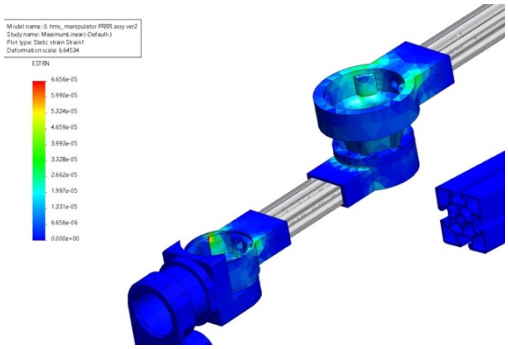

Figure 10: Highest strain distribution

Fabricated Prototype

Once the evaluation of the design is finished and it is determined to be safe, the robotic arm will be manufactured using 3D printing. In 3D printing, the strength of printed parts will depend on the infill density of the filament [3]. 100% infill density indicates that the printed parts are solid and less dense meaning the parts will be hollow. However, higher infill density will require more filament to be used and therefore increase the cost to fabricate. In this robotic arm, the parts were printed with 50% infill density which is sufficient density for the prototype[4]. Figure 11 shows the fabricated prototype of this robotic arm with an infill density of 50%.

Figure 11: Prototype of robotic arm

Conclusion

The aim is to develop a robotic arm with three degrees of freedom that would enhance the user's experience by completely automating the procedure of connecting the electric car to the charging station. An in-depth investigation of the design under the applied load offers valuable insights into the safety of the robotic arm design. The prototype has shown significant potential in terms of operational feasibility, indicating a substantial advancement in reducing the amount of manual labor needed for EV charging. Three enhancements may be implemented to optimize the design, namely, the utilization of materials with greater strength, the incorporation of height adjustment functionality, and the integration of sensor-detecting technology to enhance accuracy.

ACKNOWLEDGMENTS

This work was conducted as a part of Universiti Teknologi Malaysia (UTM) and Badan Riset Inovasi Nasional, Indonesia (BRIN) collaborative research grant vot R.J130000.7351.4B734.

REFERENCES

[1] University of Virginia, & Institute of Electrical and Electronics Engineers. (2019). 2019 Systems and Information Engineering Design Symposium (SIEDS): University of Virginia, Charlottesville, Virginia, USA, 26 April 2019.

[2] Chablat, D., Mattacchione, R., & Ottaviano, E. (2022, March). Design of a robot for the automatic charging of an electric car. Retrieved from http://arxiv.org/abs/2203.16981

[3] Mazlan, M. A., Anas, M. A., Nor Izmin, N. A., & Abdullah, A. H. (2023). Effects of infill density, wall perimeter, and layer height in fabricating 3D printing products. Materials, 16(2). https://doi.org/10.3390/ma16020695

[4] Afshar, R., Jeanne, S., & Abali, B. E. (2023). Nonlinear material modeling for mechanical characterization of 3-D printed PLA polymer with different infill densities. Applied Composite Materials, 30(3), 987–1001. https://doi.org/10.1007/s10443-023-10122-y